Mutation-dependent recessive inheritance in *NPHS2*-associated steroid-resistant nephrotic syndrome.

Kálmán Tory, Dóra K. Menyhárd, Stephanie Woerner, Fabien Nevo, Olivier Gribouval, Andrea Kerti, Pál Stráner, Christelle Arrondel, Evelyne Huynh Cong, Tivadar Tulassay, Géraldine Mollet, András Perczel, Corinne Antignac

Abbreviations: *NPHS2:* nephrosis 2, steroid-resistant ; SRNS: steroid-resistant nephrotic syndrome

Introductory paragraph

Nephrotic syndrome is the consequence of damage to the glomerular filtration barrier, and it refers to the clinical symptoms of heavy proteinuria, hypoalbuminemia, edema and hyperlipidemia. The steroidresistant form of nephrotic syndrome (SRNS) has a poor prognosis, as it often leads to end-stage renal disease (ESRD)[1,2]. Mutations in more than 20 genes have been identified in monogenic forms of SRNS, most of which encode podocyte proteins3–5. NPHS2, encoding podocin, is the most frequently mutated of these genes and is responsible for 12–18% of SRNS cases[3,6,7]. Podocin accumulates in dimeric or oligomeric forms in lipid raft microdomains at the podocyte slit diaphragm, which is the key component of the glomerular filtration barrier. On the basis of its predicted structure, podocin belongs to the stomatin protein family, with a hairpin-like intramembrane loop and intracellular N and C termini. The C-terminal portions of both stomatin and podocin are responsible for dimerization[6,8–12].

Individuals with NPHS2 mutations typically develop SRNS before 6 years of age and progress to ESRD during their first decade of life6. The phenotype can be less severe in the setting of a trans association of an NPHS2 mutation and the polymorphism c.686G>A (p.Arg229Gln, rs61747728), a genotype we hereafter denote as p.[Arg229Gln];[mut] that causes SRNS with a median age at diagnosis of 13 years (range, 0–39 years) and progression to ESRD by 26 years (range, 10–50 years)[7,13–18]. Nevertheless, the p.Arg229Gln variant in the homozygous state does not cause SRNS[19,20]. On the basis of the 15× higher allele frequency of p.Arg229Gln (357/13,006, 2.7%) than the cumulative allele frequency of the known disease-causing variants[13–18,21–43] (24/13,006, 0.18%) in the National Heart, Lung, and Blood Institute (NHLBI) exome variant server (see URLs), one would expect the prevalence of late onset SRNS secondary to p.[Arg229Gln];[mut] to exceed that of early onset SRNS secondary to two NPHS2 mutations (referred to here as [mut];[mut]) by 30× (i.e., 2rq as compared to q2, where r and q correspond to the allele frequency of p.Arg229Gln and that of the mutations, respectively). However, late onset SRNS secondary to p.[Arg229Gln];[mut] (n = 71)

was reported to be 3.5× less frequent than early onset SRNS secondary to [mut];[mut] (n = 247) in the French and other large SRNS cohorts13–18,21–43. This substantial (100×) difference between the expected and observed ratios suggested to us that p.[Arg229Gln];[mut] is not disease causing in the majority of cases.

To test this hypothesis, we screened for p.Arg229Gln in the unaffected parents of affected children with NPHS2 mutations, i.e., unaffected individuals who are obligate mutation carriers. Indeed, out of 129 parents, we found a total of 6 (4.7%), aged 42–62 years, to be compound heterozygous for alleles encoding p.Arg229Gln and one of the following alterations in trans: p.Arg138Gln, p.Arg138* (n = 2), p.Arg168His, c.534+1G>T or p.Arg238Ser. These findings clearly demonstrate the incomplete penetrance of SRNS in p.[Arg229Gln];[mut] individuals. Nevertheless, the high allele frequency of p.Arg229Gln in late onset SRNS (5.7–7.5%)[16–18] points to its pathogenicity in some cases. Recognizing that this discrepancy could reflect the influence of the trans-associated mutations, we compared the exonic localization of the mutations between cases with [mut];[mut] and cases with p.[Arg229Gln];[mut] in 318 families from French and other SRNS cohorts[13–18,21–43] and found a striking difference (P = 1.2 × 10−35; Table 1). Notably, whereas mutations in the last two exons (7 and 8) were rare in cases with [mut];[mut], these mutations were associated with p.Arg229Gln in the vast majority of cases with p.[Arg229Gln];[mut]. This difference points to a pivotal role of the trans-associated mutation in determining the pathogenicity of p.Arg229Gln.

To determine which mutations specifically were pathogenic in association with p.Arg229Gln, we compared their allele frequencies between cases with p.[Arg229Gln];[mut] and cases with [mut];[mut][13–18,21–43] (Table 2 and Supplementary Table 1). Missense mutations affecting Ala284, Ala288, Arg291, Ala297, Glu310, Leu327 or Gln328 (‘associated mutations’) were enriched in cases carrying p.[Arg229Gln];[mut], confirming the pathogenicity of their associations. In contrast, the allele encoding p.Val290Met, despite being the most common missense mutation of exons 7 and 8, was never reported in association with p.Arg229Gln, making the pathogenicity ofp.[Val290Met];[Arg229Gln] unlikely (Table 2). We indeed found two second-degree relatives of a case homozygous for p.Val290Met41 who carried [p.Val290Met];[Arg229Gln] with no proteinuria (<20 mg l−1) at the ages of 37 and 43 years, confirming its non-pathogenic nature (Supplementary Fig. 1).

Out of the 56 mutations located in exons 1–6, only 4 were associated with p.Arg229Gln in cases with SRNS, and these accounted for only 8 of 71 (11%) total p.Arg229Gln-associated alleles (Tables 1 and 2)13–18,21–43. Even these four associations are unlikely to be pathogenic for several reasons. First, we found two of the associations (p.[Arg138Gln]; [Arg229Gln] and p.[Arg238Ser];[Arg229Gln]) in

unaffected parents. Second, the phenotypesof the six cases with available clinical information (previously published[13,18] and identified in the French cohort here) suggest a non–NPHS2-related pathology, either because of interstitial calcification, tubular atrophy and hypogammaglobulinemia in one case with p.[Arg238Ser];[Arg229Gln] or because of a clinical course that is highly reminiscent of an immune-mediated process, including recurrence after transplant in three cases with p.[Arg138Gln];[Arg229Gln] or early response to steroid therapy in two cases with p.[Gln215*];[Arg229Gln] or p.[Lys126Ilefs*7];[Arg229Gln]). Third, if p.[Arg138Gln];[Arg229Gln] were pathogenic, the number of cases with this association would be expected to exceed the number of cases with p.[Arg138Gln];[mut], but we found the inverse to be true (Table 2). Thus, the rare association of a mutation in exons 1–6 and p.Arg229Gln in 8 of 3,004 (0.3%) families with SRNS[13–18,21–43] is very likely to be an incidental finding without a causal role. Notably, the cumulative allele frequency of the associated mutations among all mutated alleles in cases with [mut];[mut] (9/494 alleles, 1.8%; Table 2) is in agreement with the 100× difference between the expected and observed prevalence of cases with p.[Arg229Gln];[mut]. Nevertheless, it cannot be excluded that other rare mutations of exons 7 and 8 are also pathogenic when associated with p.Arg229Gln (Table 2). As all the associated mutations were C-terminal substitutions, we hypothesized that they exert a deleterious effect on p.Arg229Gln podocin. We therefore studied the membrane targeting of p.Arg229Gln podocin in human podocyte cell lines transiently coexpressing different podocin constructs. In perfect accordance with the clinical data, p.Arg229Gln podocin was localized properly to the plasma membrane when coexpressed with wild-type podocin, p.Arg238Ser podocin or p.Val290Met podocin but was retained in the cytoplasm when coexpressed with p.Ala284Val, p.Ala288Thr, p.Arg291Trp, p.Ala297Val or p.Glu310Lys podocin (Supplementary Fig. 2). These latter podocin mutants showed a reticular and dispersed vesicular localization pattern similar to that of p.Arg291Trp podocin that is known to be trapped in the endoplasmic reticulum (ER) and vesicles11,44 and did not markedly modify the localization of coexpressed wild-type podocin (Supplementary Fig. 2). Furthermore, p.Arg138Gln podocin, which is known to be retained in the ER[10,11,44,45], did not alter the localization of p.Arg229Gln podocin, which is in accordance with the non-pathogenic nature of their association (Supplementary Fig. 2). We found similar results in podocytes stably coexpressing wild-type podocin or p.Arg229Gln podocin with podocin mutants (Fig. 1). Notably, we also confirmed the non-membrane targeting of endogenous podocin in podocytes isolated from urine of a case with p.[Arg229Gln];[Ala284Val], a result that is contrary to its membranous localization in control patients with p.[Arg229Gln];[=]

(Fig. 2 and Supplementary Fig. 3). Thus, all the clinical observations, in vitro studies and ex vivo studies strongly support a deleterious effect of certain podocin mutants on p.Arg229Gln podocin, mimicking a dominant-negative effect.

To understand this interaction at an atomic resolution, we examined the calculated structure of their dimers. On the basis of structural modeling, the homodimer of the C-terminal fragment (residues 161–383) of wild-type podocin consists of two head domains (residues161–270) connected by their intertwined helical tails (residues

271–332), forming a coiled-coil–type association (Fig. 3a). Arg229 is stabilized in the core of the globular head domain by at least two hydrogen bonds involving Glu233, Glu237 or Asp244 (Fig. 3b).

In p.Arg229Gln podocin, Glu233 and Glu237 are released from these contacts, flip toward the helical tail domain and form electrostatic interactions with Arg286 and Lys289, rigidifying the structure by forming an additional head-tail interaction (Fig. 3b,c). Nevertheless, both the p.Arg229Gln podocin homodimer and the heterodimer of p.Val290Met podocin with p.Arg229Gln podocin formed a topologically similar molecular arrangement to that of the wild-type homodimer (Fig. 4a). Moreover, the structure of the heterodimer of p.Ala284Val podocin with wild-type podocin was highly reminiscent of that of the wild-type podocin homodimer as well (Fig. 4a). In contrast, heterodimers of p.Ala284Val podocin with p.Arg229Gln podocin and of p.Ala297Val podocin with p.Arg229Gln podocin, as well as the p.Ala284Val podocin homodimer, showed characteristically different structures (Fig. 4b), which is in keeping with their pathogenicities. The derived structures support the conclusion that the combination of the p.Arg229Gln variant with the associated mutations leads to an altered mode of dimerization, which we propose contributes to the retention of p.Arg229Gln podocin within cytoplasmic compartments.

The role of the associated mutations in the pathogenicity of p.Arg229Gln can explain several clinical observations: (i) the difference between the observed and expected prevalence of cases with p.[Arg229Gln];[mut]; (ii) the steroid sensitivity of nephrotic syndrome in a case with p.[Arg229Gln];[truncating mutation][24]; (iii) the lack of pseudo-dominant inheritance in families with NPHS2 mutations in exons 1–6 despite the non-negligible allele frequency of p.Arg229Gln[13–18,21–43]; and (iv) the late onset nature of SRNS in cases with p.[Arg229Gln];[mut][16–18], as p.Arg229Gln podocin homodimers are still expected to function properly.

In conclusion, the NPHS2 allele encoding p.Arg229Gln is only pathogenic when associated with specific mutations. Thus, we describe an autosomal-recessive disorder in which the pathogenicity of one allele depends on that of the other. This phenomenon has direct clinical implications. Unlike current counseling practices, a couple carrying an NPHS2 mutation located in exons 1–6 in one

member and p.Arg229Gln in the other are not at risk of having an affected child. Conversely, genetic counseling of couples with p.Arg229Gln and associated mutations will be challenging, as the potential transmission rate of 50% for two unaffected parents, or the potential transmission rates of 25%, 75% or 100% for an affected and an unaffected parent, are not expected in autosomal-recessive disorders (Supplementary Fig. 4). Other autosomal-recessive disorders may also be inherited in such a mutation-dependent recessive fashion, especially if the encoded protein forms oligomers. In this study, we provide an example of how common variants can be implicated in rare monogenic diseases, thus opening a new aspect in the assessment of the pathogenicity of sequence variants.

Acknowledgement

We thank S. Lyonnet, L. Abel, S. Harvey and M. Muorah for careful reading and discussion of the manuscript and M. Saleem (Bristol Royal Hospital for Children, University of Bristol) for providing the podocyte cell line. We acknowledgeE. Jávorszky, M. Bernáth, M. Krámer and Zs. Nagy for providing assistance, N. Goudin of the Necker Institute Imaging Facility for providing expert knowledge on confocal microscopy, G. Froment, D. Nègre and C. Costa for production of lentivectors (Structure Fédérative de Recherche BioSciences Gerland–Lyon Sud–UMS3444/US8) and the National Information Infrastructure Development Institute (NIIFI) supercomputing center (Hungary). We thank the patients and their family members for participation. Financial support for this work was provided by grants from the Fondation pour la Recherche Médicale (project DMP 2010-11-20-386 to C. Antignac), the Agence Nationale de la Recherche (GenPod project ANR-12-BSV1-0033.01 and 'Investments for the Future' program ANR-10-IAHU-01, both to C. Antignac), the European Community's 7th Framework program grant 2012-305608 (Eurenomics) to C. Antignac, Fondation Association pour la Recherche sur le Cancer (ARC) TÁMOP-4.2.1/B-09/1/KMR-2010-0001 to K.T., OTKA 84087/2010 to T.T., Hungarian Scientific Research Fund (OTKA NK101072 to A.P., K109718 to K.T. and PD101095 to D.K.M.) and a Bolyai János research fellowship of the Hungarian Academy of Sciences to K.T.

Table 1. Distribution of *NPHS2* mutations in patients with [Arg229Gln];[mut] and in patients with [mut];[mut] (n: number of mutated alleles)

	[Arg229Gln];[mut] Total of 71 patients		[mut];[mut] Total of 247 patients		
	n	ratio	*n*	ratio	*p*
exons 1-6	8	11.3%	421	85.2%	3.8×10^{-36}

exons 7-8	63	88.7%	73	14.8%

Table 2. Allele frequency of *NPHS2* mutations in patients with [p.Arg229Gln];[mut] and in patients with ([mut];[mut])

		patients with [Arg229Gln];[mut]		patients with [mut];[mut]		
	mutations	*n*	ratio	*n*	ratio	*p*
exons 1-6	Lys126Ilefs*7	1	1.4%	0		0.12
	Arg138Gln [a]	5	7.0%	171	34.6%	3.9×10^{-7}
	Gln215*	1	1.4%	6	1.2%	1
	Arg238Ser [a]	1	1.4%	3	0.6%	0.42
	all the other mutations in exons 1-6 (n=53 type) [b]	0		241	48.8%	2.1×10^{-19}
exon 7	p.Val268Asp*16	0		2	0.4%	1
	p.Leu270Phe	1	1.4%	0	0.0%	0.12
	p.Pro271Leu	0		1	0.2%	1
	p.His276Leu	0		2	0.4%	1
	p.His276Alafs*8	0		2	0.4%	1
	p.Glu281Ala	0		2	0.4%	1
	p.Ala284Val	26	36.6%	8 [c]	1.6%	3.3×10^{-19}
	p.Arg286Thrfs*17	3	4.2%	20	4.0%	1
	p.Ala288Thr	4	5.6%	0		0.0002
	p.Lys289*	0		2	0.4%	1
	p.Val290Met	0		13	2.6%	0.39
	p.Arg291Trp	4	5.6%	1	0.2%	0.001
	c.873+2T>A	0		1	0.2%	1
	c.873+5G>A	0		2	0.4%	1
exon 8	c.874-1G>C	0		2	0.4%	1
	p.Ala295Thr	1	1.4%	0		0.12
	p.Ala297Val	4	5.6%	0		0.0002
	p.Ala300Pro	1	1.4%	0		0.12
	p.A301del	0		4	0.8%	1
	p.Leu305Pro	1	1.4%	0		0.12
	p.Glu310Ala	1	1.4%	0		0.12
	p.Glu310Lys	5	7.0%	0		2.8×10^{-5}
	p.Glu310Val	2	2.8%	0		0.016
	p.Glu310 total					4.3×10^{-8}
	p.Ala317Leufs*31	1	1.4%	7	1.4%	1
	p.Leu321Phefs*27	1	1.4%	0		0.12
	p.Arg322Gly	1	1.4%	2	0.4%	0.33
	p.Leu324GludelinsHis	0		1	0.2%	1
	p.Leu327Phe	3	4.2%	0		0.002
	p.Gln328Arg	2	2.8%	0		0.016
	p.Phe344Leufs*4	1	1.4%	0		0.12
	p.Leu346Tyrfs*2	1	1.4%	0		0.12

	p.Pro372Ilefs*16	0		1	0.2%	1
	Total:	71	100%	494	100%	

[a]: these two mutations were also found in unaffected parents in trans-association with Arg229Gln, [b]: detailed in Supplementary data, [c]: eight alleles of four homozygous patients. Mutations significantly enriched in patients with [p.Arg229Gln];[mut] are in gray, mutations enriched in patients with ([mut];[mut]) are in yellow

References

1. Mekahli, D. et al. Long-term outcome of idiopathic steroid-resistant nephrotic syndrome: a multicenter study. Pediatr. Nephrol. 24, 1525–1532 (2009).
2. Tune, B.M. & Mendoza, S.A. Treatment of the idiopathic nephrotic syndrome: regimens and outcomes in children and adults. J. Am. Soc. Nephrol. 8, 824–832 (1997).
3. Benoit, G., Machuca, E. & Antignac, C. Hereditary nephrotic syndrome: a systematic approach for genetic testing and a review of associated podocyte gene mutations. Pediatr. Nephrol. 25, 1621–1632 (2010).
4. Mele, C. et al. MYO1E mutations and childhood familial focal segmental glomerulosclerosis. N. Engl. J. Med. 365, 295–306 (2011).
5. Akilesh, S. et al. Arhgap24 inactivates Rac1 in mouse podocytes, and a mutant form is associated with familial focal segmental glomerulosclerosis. J. Clin. Invest. 121, 4127–4137 (2011).
6. Boute, N. et al. NPHS2, encoding the glomerular protein podocin, is mutated in autosomal recessive steroid-resistant nephrotic syndrome. Nat. Genet. 24, 349–354 (2000).
7. Santín, S. et al. Clinical utility of genetic testing in children and adults with steroid-resistant nephrotic syndrome. Clin. J. Am. Soc. Nephrol. 6, 1139–1148 (2011).
8. Schwarz, K. et al. Podocin, a raft-associated component of the glomerular slit diaphragm, interacts with CD2AP and nephrin. J. Clin. Invest. 108, 1621–1629 (2001).
9. Huber, T.B., Kottgen, M., Schilling, B., Walz, G. & Benzing, T. Interaction with podocin facilitates nephrin signaling. J. Biol. Chem. 276, 41543–41546 (2001).
10. Huber, T.B. et al. Molecular basis of the functional podocin-nephrin complex: mutations in the NPHS2 gene disrupt nephrin targeting to lipid raft microdomains. Hum. Mol. Genet. 12, 3397–3405 (2003).
11. Roselli, S., Moutkine, I., Gribouval, O., Benmerah, A. & Antignac, C. Plasma membrane targeting of podocin through the classical exocytic pathway: effect of NPHS2 mutations. Traffic 5, 37–44 (2004).
12. Snyers, L., Umlauf, E. & Prohaska, R. Oligomeric nature of the integral membrane protein stomatin. J. Biol. Chem. 273, 17221–17226 (1998).
13. Berdeli, A. et al. NPHS2 (podocin) mutations in Turkish children with idiopathic nephrotic syndrome. Pediatr. Nephrol. 22, 2031–2040 (2007).
14. Hinkes, B. et al. Specific podocin mutations correlate with age of onset in steroid-resistant nephrotic syndrome. J. Am. Soc. Nephrol. 19, 365–371 (2008).
15. Ruf, R.G. et al. Patients with mutations in NPHS2 (podocin) do not respond to standard steroid treatment of nephrotic syndrome. J. Am. Soc. Nephrol. 15,
722–732 (2004).
16. Machuca, E. et al. Clinical and epidemiological assessment of steroid-resistant nephrotic syndrome associated with the NPHS2 R229Q variant. Kidney Int. 75, 727–735 (2009).
17. Tsukaguchi, H. et al. NPHS2 mutations in late-onset focal segmental glomerulosclerosis: R229Q is a common disease-associated allele. J. Clin. Invest. 110, 1659–1666 (2002).
18. Tonna, S.J. et al. NPHS2 variation in focal and segmental glomerulosclerosis. BMC Nephrol. 9, 13 (2008).
19. Kerti, A. et al. NPHS2 homozygous p.R229Q variant: potential modifier instead

of causal effect in focal segmental glomerulosclerosis. Pediatr. Nephrol. 28,
2061–2064 (2013).
20. Köttgen, A. et al. The association of podocin R229Q polymorphism with increased albuminuria or reduced estimated GFR in a large population-based sample of US adults. Am. J. Kidney Dis. 52, 868–875 (2008).
21. Santín, S. et al. Clinical value of NPHS2 analysis in early- and adult-onset steroid-resistant nephrotic syndrome. Clin. J. Am. Soc. Nephrol. 6, 344–354 (2011).
22. Büscher, A.K. et al. Immunosuppression and renal outcome in congenital and pediatric steroid-resistant nephrotic syndrome. Clin. J. Am. Soc. Nephrol. 5,
2075–2084 (2010).
23. Caridi, G. et al. Prevalence, genetics, and clinical features of patients carrying podocin mutations in steroid-resistant nonfamilial focal segmental glomerulosclerosis. J. Am. Soc. Nephrol. 12, 2742–2746 (2001).
24. He, N. et al. Recessive NPHS2 (Podocin) mutations are rare in adult-onset idiopathic focal segmental glomerulosclerosis. Clin. J. Am. Soc. Nephrol. 2, 31–37 (2007).
25. Hinkes, B.G. et al. Nephrotic syndrome in the first year of life: two thirds of cases are caused by mutations in 4 genes (NPHS1, NPHS2, WT1, and LAMB2). Pediatrics 119, e907–e919 (2007).
26. Ismaili, K. et al. Genetic forms of nephrotic syndrome: a single-center experience in Brussels. Pediatr. Nephrol. 24, 287–294 (2009).
27. Karle, S.M. et al. Novel mutations in NPHS2 detected in both familial and sporadic steroid-resistant nephrotic syndrome. J. Am. Soc. Nephrol. 13, 388–393 (2002).
28. Kitamura, A. et al. Steroid-resistant nephrotic syndrome. Kidney Int. 74,
1209–1215 (2008).
29. Machuca, E. et al. Genotype-phenotype correlations in non-Finnish congenital nephrotic syndrome. J. Am. Soc. Nephrol. 21, 1209–1217 (2010).
30. Megremis, S. et al. Nucleotide variations in the NPHS2 gene in Greek children with steroid-resistant nephrotic syndrome. Genet. Test. Mol. Biomarkers 13,
249–256 (2009).
31. Monteiro, E.J., Pereira, A.C., Pereira, A.B., Krieger, J.E. & Mastroianni-Kirsztajn, G. NPHS2 mutations in adult patients with primary focal segmental glomerulosclerosis. J. Nephrol. 19, 366–371 (2006).
32. Nakatsue, T. et al. Nephrin and podocin dissociate at the onset of proteinuria in experimental membranous nephropathy. Kidney Int. 67, 2239–2253 (2005).
33. Sako, M. et al. Analysis of NPHS1, NPHS2, ACTN4, and WT1 in Japanese patients with congenital nephrotic syndrome. Kidney Int. 67, 1248–1255 (2005).
34. Schultheiss, M. et al. No evidence for genotype/phenotype correlation in NPHS1 and NPHS2 mutations. Pediatr. Nephrol. 19, 1340–1348 (2004).
35. Skálová, S., Podhola, M., Vondrak, K. & Chernin, G. Plasmapheresis-induced clinical improvement in a patient with steroid-resistant nephrotic syndrome due to podocin (NPHS2) gene mutation. Acta Medica (Hradec Kralove) 53, 157–159 (2010).
36. Voskarides, K. et al. NPHS2 screening with SURVEYOR in Hellenic children with steroid-resistant nephrotic syndrome. Pediatr. Nephrol. 23, 1373–1375 (2008).
37. Weber, S. et al. NPHS2 mutation analysis shows genetic heterogeneity of steroid-resistant nephrotic syndrome and low post-transplant recurrence. Kidney Int. 66, 571–579 (2004).
38. Yu, Z. et al. Mutations in NPHS2 in sporadic steroid-resistant nephrotic syndrome in Chinese children. Nephrol. Dial. Transplant. 20, 902–908 (2005).
39. Koziell, A. et al. Genotype/phenotype correlations of NPHS1 and NPHS2 mutations in nephrotic syndrome advocate a functional inter-relationship in glomerular filtration. Hum. Mol. Genet. 11, 379–388 (2002).

40. Sun, H. et al. A novel mutation in NPHS2 gene identified in a Chinese pedigree with autosomal recessive steroid-resistant nephrotic syndrome. Pathology 41, 661–665 (2009).
41. Kerti, A. et al. NPHS2 p.V290M mutation in late-onset steroid-resistant nephrotic syndrome. Pediatr. Nephrol. 28, 751–757 (2013).
42. Mbarek, I.B. et al. Novel mutations in steroid-resistant nephrotic syndrome diagnosed in Tunisian children. Pediatr. Nephrol. 26, 241–249 (2011).
43. Jungraithmayr, T.C. et al. Screening for NPHS2 mutations may help predict FSGS recurrence after transplantation. J. Am. Soc. Nephrol. 22, 579–585 (2011).
44. Nishibori, Y. et al. Disease-causing missense mutations in NPHS2 gene alter normal nephrin trafficking to the plasma membrane. Kidney Int. 66, 1755–1765 (2004).
45. Ohashi, T., Uchida, K., Uchida, S., Sasaki, S. & Nihei, H. Intracellular mislocalization of mutant podocin and correction by chemical chaperones. Histochem. Cell Biol. 119, 257–264 (2003).

Figure 1.

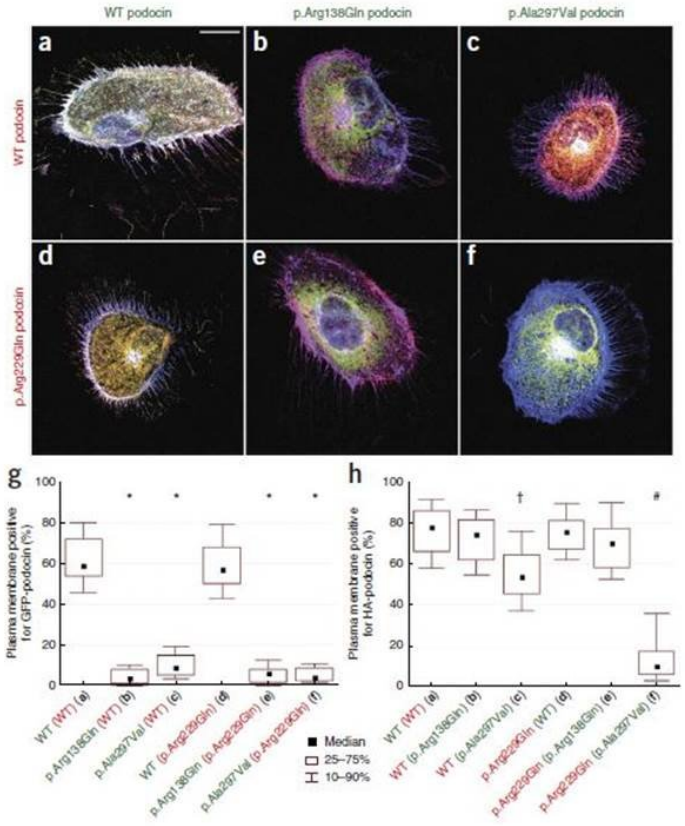

Figure 1. Membrane targeting of wild-type podocin and p.Arg229Gln podocin as a function of the associated mutation in podocytes stably coexpressing podocin mutants. (a–f) Hemagglutinin (HA)-tagged wild-type (WT) (a–c) and p.Arg229Gln (d–f) podocin are shown in red, and the coexpressed GFP-tagged podocin proteins are shown in green. The plasma membrane is labeled with wheat germ agglutinin (WGA) and shown in blue. Both wild-type and p.Arg229Gln podocin are localized to the plasma membrane when coexpressed with wild-type podocin (a,d, white pixels correspond to the merge of red, green and blue) and with p.Arg138Gln podocin, despite the retention of the latter protein in the ER (b,e, magenta pixels correspond to the merge of red and blue). Although membrane targeting of wild-type podocin is only moderately decreased in cells coexpressing p.Ala297Val podocin (c, magenta pixels), that of p.Arg229Gln podocin is abolished (f). Scale bar, 20 μm. (g,h) Membrane targeting of podocin proteins quantified as the percentage of the plasma membrane (WGA) that is positive for GFP-tagged (g) or HA-tagged (h) podocin proteins within 30 cells per group. GFP-tagged and HA-tagged podocin proteins are indicated in green and red, respectively. The coexpressed podocin proteins are in parentheses, followed by the panel label corresponding to each quantification. $^{*}P < 3.3 \times 10^{-11}$ as compared to WT (WT-GFP); $^{\dagger}P = 1.8 \times 10^{-6}$ as compared to WT (WT-HA); $^{\#}P = 3.5 \times 10^{-11}$ as compared to p.Arg229Gln (WT).

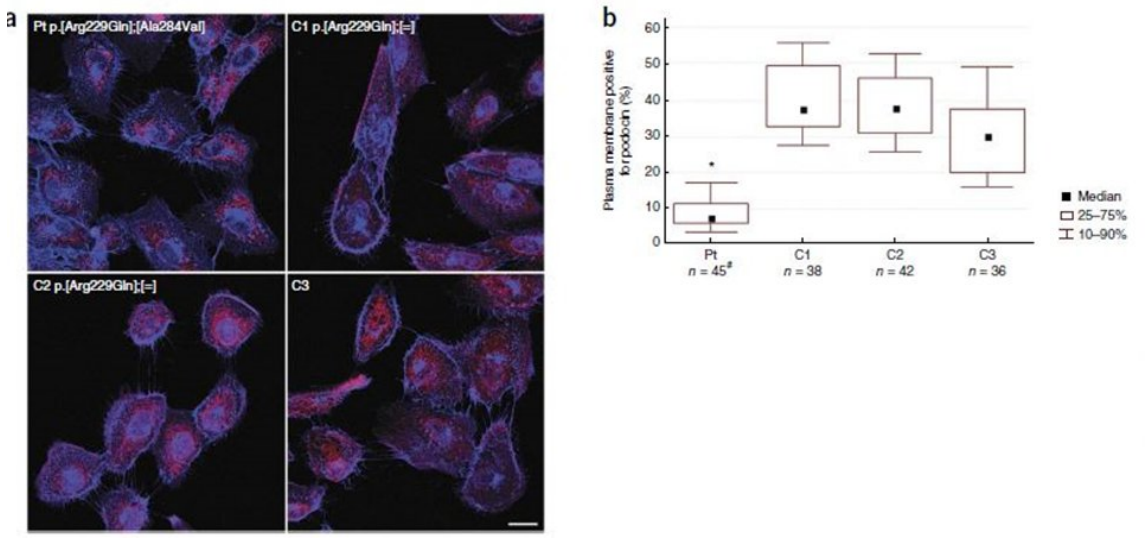

Figure 2. Membrane targeting of endogenous podocin in urinary podocytes of cases with SRNS carrying p.Arg229Gln. (a) Endogenous podocin is shown in red, and the WGA-labeled plasma membrane is shown in blue. Podocin is well targeted to the plasma membrane in the three control patients with non–*NPHS2*-associated glomerulopathy (C1–C3), two of whom are heterozygous carriers of p.Arg229Gln, in contrast to the patient with p.[Arg229Gln];[Ala284Val] (Pt). Scale bar, 20 µm. (b) Membrane targeting of podocin proteins shown as the percentage of the plasma membrane (WGA) that is positive for endogenous podocin. The *n* values below each patient indicate the number of cells quantified. #45 cells quantified in three different immunostaining experiments on two different cultures of urinary podocytes; $*P \leq 6.7 \times 10^{-13}$ as compared to each of the three control patients.

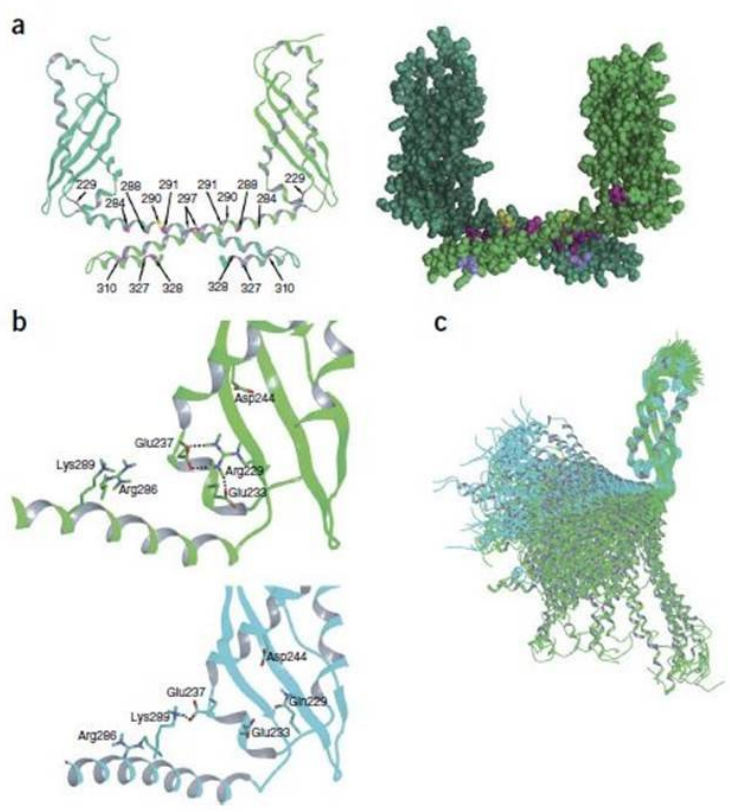

Figure 3. Structure of the wild-type podocin homodimer and the effect of p.Arg229Gln. (a) Calculated structure of the wild-type podocin homodimer (monomers A and B are in light and dark green, respectively) shown as ribbon diagram (left) and an all-atom representation (excluding non-polar H atoms for clarity; right). Altered residues that point inward to the head domain (229) and the coiled-coil region (284, 288, 291, 297 and 328) are colored magenta on both monomers. Alterations at these latter positions are expected to impair the mode of dimerization, in contrast to Val290 (yellow), which points outward from the coiled-coiled domain. Glu310 and Leu327 (lilac) seem like fenders to the coiled-coil region: Glu310 participates in a charge network of Glu296, Lys299, Glu303, Arg306 and Glu310, creating a − + − + − charge motif at the surface of the molecule, whereas at the opposite side, Leu327 is part of a hydrophobic patch. (b,c) The H-bond network stabilizing Arg229 within the head domain of wild-type podocin (green) is rearranged in the p.Arg229Gln mutant (cyan) (b) and restricts the pliability of the overall conformation of p.Arg229Gln podocin (cyan) compared to that of the wild-type podocin monomer (in green) (c). c is an ensemble of characteristic conformations sampled in the last 10 ns of the simulation.

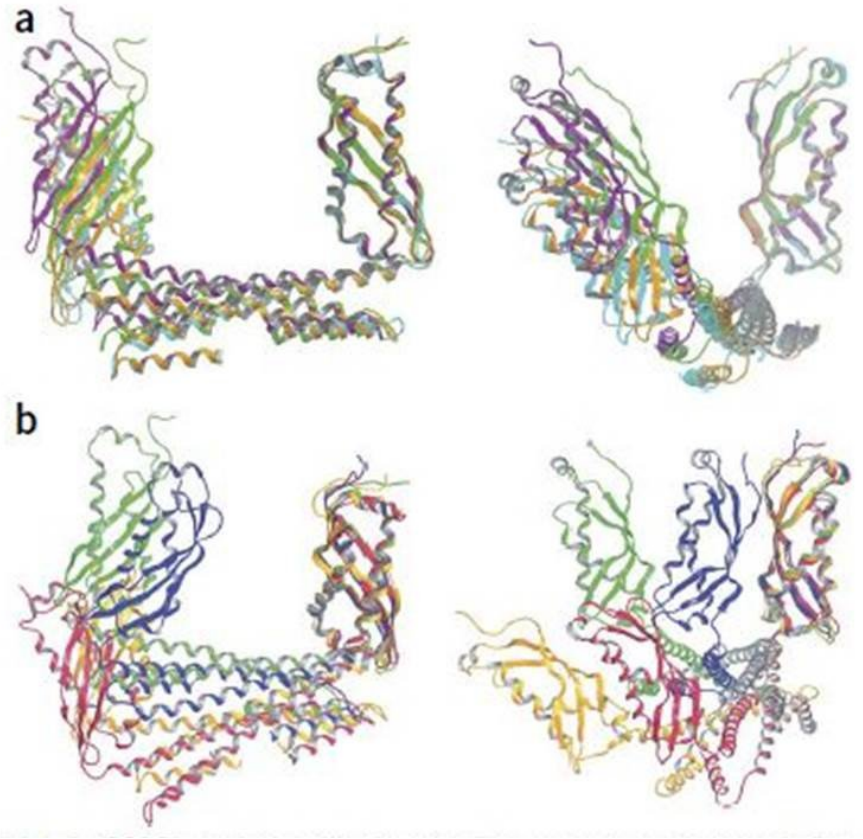

Figure 4. Superimposed average structures of the non-pathogenic and pathogenic dimers. Frontal and lateral structural views of podocin dimers are shown overlaid based on their globular region of monomer A for comparison. (a) Non-pathogenic dimers of p.Arg229Gln with p.Arg229Gln podocin (cyan), p.Val290Met with p.Arg229Gln podocin (orange) and p.Ala284Val with wild-type podocin (purple) are similar in structure to the wild-type podocin homodimer (green). (b) The structures in a are in contrast to the structures formed by the pathogenic dimers of p.Ala284Val with p.Arg229Gln podocin (red) and p.Ala297Val with p.Arg229Gln podocin (yellow) and the p.Ala284Val and p.Ala284Val podocin homodimer (blue) shown superimposed on the wild-type podocin homodimer (green). Accordingly, the root mean square deviations of the backbone atoms compared to those in wild-type podocin were 2.7 Å, 2.9 Å and 3.3 Å for the non-pathogenic dimers shown in a, respectively, and 4.9 Å, 6.9 Å and 9.5 Å for the pathogenic dimers shown in b, respectively. Mobility of the backbone atoms (reflecting the well-defined nature of the structure) remained similar: the mobility was slightly decreased (~30%) in both the dimers of p.Arg229Gln with p.Arg229Gln podocin and p.Val290Met with p.Arg229Gln podocin and was increased (~20%) in the dimer of p.Ala284Val with wild-type podocin with respect to wild-type podocin. A slight increase in mobility is seen for the pathogenic dimer of p.Ala284Val with p.Ala284Val podocin (~24%) as well, which is accompanied by the largest root mean square deviation from the wild-type dimer. This indicates a stabilized but quite altered three-dimensional structural arrangement. With respect to the wild-type dimer, the remaining pathogenic dimers, p.Ala284Val with p.Arg229Gln podocin and p.Ala297Val with p.Arg229Gln podocin, show intermediate root mean square deviations but a striking increase (~140%) in mobility, resulting in conformational states that are markedly different from that of wild-type podocin.